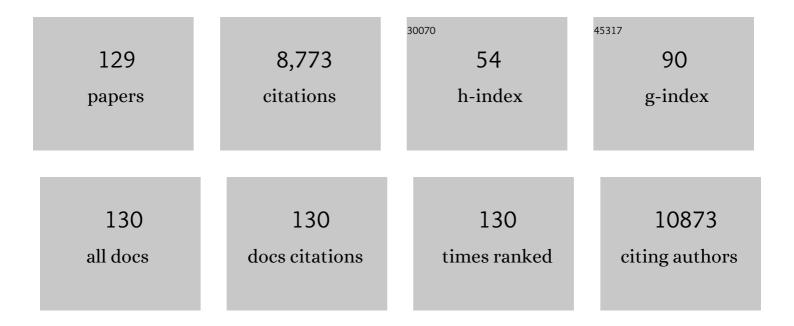
List of Publications by Year in descending order

Source: https://exaly.com/author-pdf/8530685/publications.pdf Version: 2024-02-01



#	Article	IF	CITATIONS
1	Enabling Superior Electrochemical Properties for Highly Efficient Potassium Storage by Impregnating Ultrafine Sb Nanocrystals within Nanochannelâ€Containing Carbon Nanofibers. Angewandte Chemie - International Edition, 2019, 58, 14578-14583.	13.8	332
2	Ru Modulation Effects in the Synthesis of Unique Rod-like Ni@Ni <sub>2</sub> P–Ru Heterostructures and Their Remarkable Electrocatalytic Hydrogen Evolution Performance. Journal of the American Chemical Society, 2018, 140, 2731-2734.	13.7	326
3	Confining SnS2 Ultrathin Nanosheets in Hollow Carbon Nanostructures for Efficient Capacitive Sodium Storage. Joule, 2018, 2, 725-735.	24.0	324
4	Rice husk-derived hard carbons as high-performance anode materials for sodium-ion batteries. Carbon, 2018, 127, 658-666.	10.3	294
5	A Yolk–Shellâ€&tructured FePO <sub>4</sub> Cathode for Highâ€Rate and Longâ€Cycling Sodiumâ€lon Batteries. Angewandte Chemie - International Edition, 2020, 59, 17504-17510.	13.8	275
6	Co <sub>3</sub> S <sub>4</sub> porous nanosheets embedded in graphene sheets as high-performance anode materials for lithium and sodium storage. Journal of Materials Chemistry A, 2015, 3, 6787-6791.	10.3	247
7	2D Electron Gas and Oxygen Vacancy Induced High Oxygen Evolution Performances for Advanced Co <sub>3</sub> O <sub>4</sub> /CeO <sub>2</sub> Nanohybrids. Advanced Materials, 2019, 31, e1900062.	21.0	242
8	A Yolk–Shellâ€&tructured FePO <sub>4</sub> Cathode for Highâ€Rate and Long ycling Sodiumâ€lon Batteries. Angewandte Chemie, 2020, 132, 17657-17663.	2.0	191
9	Wet milled synthesis of an Sb/MWCNT nanocomposite for improved sodium storage. Journal of Materials Chemistry A, 2013, 1, 13727.	10.3	188
10	Electrochemiluminescence for Electric-Driven Antibacterial Therapeutics. Journal of the American Chemical Society, 2018, 140, 2284-2291.	13.7	180
11	Metal–organic framework templated nitrogen and sulfur co-doped porous carbons as highly efficient metal-free electrocatalysts for oxygen reduction reactions. Journal of Materials Chemistry A, 2014, 2, 6316-6319.	10.3	179
12	Heteroatoms ternary-doped porous carbons derived from MOFs as metal-free electrocatalysts for oxygen reduction reaction. Scientific Reports, 2014, 4, 5130.	3.3	174
13	Defectâ€Rich Ni <sub>3</sub> FeN Nanocrystals Anchored on Nâ€Doped Graphene for Enhanced Electrocatalytic Oxygen Evolution. Advanced Functional Materials, 2018, 28, 1706018.	14.9	169
14	Polyoxometalate-based metal–organic framework-derived hybrid electrocatalysts for highly efficient hydrogen evolution reaction. Journal of Materials Chemistry A, 2016, 4, 1202-1207.	10.3	165
15	Fluorine-Doped Carbon Particles Derived from Lotus Petioles as High-Performance Anode Materials for Sodium-Ion Batteries. Journal of Physical Chemistry C, 2015, 119, 21336-21344.	3.1	158
16	Kelp-derived hard carbons as advanced anode materials for sodium-ion batteries. Journal of Materials Chemistry A, 2017, 5, 5761-5769.	10.3	143
17	A Chemically Coupled Antimony/Multilayer Graphene Hybrid as a High-Performance Anode for Sodium-Ion Batteries. Chemistry of Materials, 2015, 27, 8138-8145.	6.7	139
18	A selenium-confined microporous carbon cathode for ultrastable lithium–selenium batteries. Journal of Materials Chemistry A, 2014, 2, 17735-17739.	10.3	117

#	Article	IF	CITATIONS
19	Cesium Lead Halide Perovskite Quantum Dots as a Photoluminescence Probe for Metal Ions. Advanced Materials, 2017, 29, 1700150.	21.0	112
20	Cobalt Phosphides Nanocrystals Encapsulated by Pâ€Doped Carbon and <i>Married</i> with Pâ€Doped Graphene for Overall Water Splitting. Small, 2019, 15, e1804546.	10.0	110
21	Template-free synthesis of metal oxide hollow micro-/nanospheres <i>via</i> Ostwald ripening for lithium-ion batteries. Journal of Materials Chemistry A, 2018, 6, 10168-10175.	10.3	109
22	Heterostructural CsPbX <sub>3</sub> -PbS (X = Cl, Br, I) Quantum Dots with Tunable Vis–NIR Dual Emission. Journal of the American Chemical Society, 2020, 142, 4464-4471.	13.7	107
23	A Few-Layer SnS2/Reduced Graphene Oxide Sandwich Hybrid for Efficient Sodium Storage. Journal of Physical Chemistry C, 2017, 121, 3261-3269.	3.1	105
24	An SbO <sub><i>x</i></sub> /Reduced Graphene Oxide Composite as a High-Rate Anode Material for Sodium-Ion Batteries. Journal of Physical Chemistry C, 2014, 118, 23527-23534.	3.1	101
25	Photocatalytic Activity of (Copper, Nitrogen)â€Codoped Titanium Dioxide Nanoparticles. Journal of the American Ceramic Society, 2008, 91, 1369-1371.	3.8	100
26	Electrochemiluminescence Tuned by Electron–Hole Recombination from Symmetry-Breaking in Wurtzite ZnSe. Journal of the American Chemical Society, 2016, 138, 1154-1157.	13.7	96
27	Integrating ultrathin and modified NiCoAl-layered double-hydroxide nanosheets with N-doped reduced graphene oxide for high-performance all-solid-state supercapacitors. Nanoscale, 2019, 11, 9896-9905.	5.6	95
28	Fluorescence Regulation of Poly(thymine)-Templated Copper Nanoparticles via an Enzyme-Triggered Reaction toward Sensitive and Selective Detection of Alkaline Phosphatase. Analytical Chemistry, 2017, 89, 3681-3686.	6.5	93
29	Ge Nanoparticles Encapsulated in Nitrogen-Doped Reduced Graphene Oxide as an Advanced Anode Material for Lithium-Ion Batteries. Journal of Physical Chemistry C, 2014, 118, 28502-28508.	3.1	92
30	Aggregation of Individual Sensing Units for Signal Accumulation: Conversion of Liquid-Phase Colorimetric Assay into Enhanced Surface-Tethered Electrochemical Analysis. Journal of the American Chemical Society, 2015, 137, 8880-8883.	13.7	92
31	Synthesis and magnetic behavior of an array of nickel-filled carbon nanotubes. Applied Physics Letters, 2002, 81, 4592-4594.	3.3	91
32	Coralloid Co <sub>2</sub> P <sub>2</sub> O <sub>7</sub> Nanocrystals Encapsulated by Thin Carbon Shells for Enhanced Electrochemical Water Oxidation. ACS Applied Materials & Interfaces, 2016, 8, 22534-22544.	8.0	91
33	Improving the Anode Performance of WS <sub>2</sub> through a Self-Assembled Double Carbon Coating. Journal of Physical Chemistry C, 2015, 119, 15874-15881.	3.1	90
34	Candied-Haws-like Architecture Consisting of FeS <sub>2</sub> @C Core–Shell Particles for Efficient Potassium Storage. , 2021, 3, 356-363.		90
35	Ultrathin palladium nanosheets with selectively controlled surface facets. Chemical Science, 2018, 9, 4451-4455.	7.4	89
36	An efficient sodium-ion battery consisting of reduced graphene oxide bonded Na3V2(PO4)3 in a composite carbon network. Journal of Alloys and Compounds, 2018, 767, 131-140.	5.5	86

#	Article	IF	CITATIONS
37	Dual Signal Amplification Using Gold Nanoparticles-Enhanced Zinc Selenide Nanoflakes and P19 Protein for Ultrasensitive Photoelectrochemical Biosensing of MicroRNA in Cell. Analytical Chemistry, 2016, 88, 10459-10465.	6.5	85
38	Chemical bonding between antimony and ionic liquid-derived nitrogen-doped carbon for sodium-ion battery anode. Journal of Power Sources, 2017, 349, 37-44.	7.8	85
39	Facile synthesis of high-quality nano-sized CdS hollow spheres and their application in electrogenerated chemiluminescence sensing. Journal of Materials Chemistry, 2007, 17, 1087-1093.	6.7	83
40	Hierarchical Nanospheres Constructed by Ultrathin MoS <sub>2</sub> Nanosheets Braced on Nitrogen-Doped Carbon Polyhedra for Efficient Lithium and Sodium Storage. ACS Applied Materials & Interfaces, 2019, 11, 2112-2119.	8.0	83
41	Uniformly-distributed Sb nanoparticles in ionic liquid-derived nitrogen-enriched carbon for highly reversible sodium storage. Journal of Materials Chemistry A, 2017, 5, 13411-13420.	10.3	79
42	Engineering Zn <sub>1–<i>x</i></sub> Cd <sub><i>x</i></sub> S/CdS Heterostructures with Enhanced Photocatalytic Activity. ACS Applied Materials & Interfaces, 2016, 8, 14535-14541.	8.0	73
43	Fe-Porphyrin-Based Covalent Organic Framework As a Novel Peroxidase Mimic for a One-Pot Glucose Colorimetric Assay. ACS Applied Bio Materials, 2018, 1, 382-388.	4.6	72
44	A facile synthesis of PdCo bimetallic hollow nanospheres and their application to Sonogashira reaction in aqueous media. New Journal of Chemistry, 2006, 30, 832.	2.8	71
45	Concave octahedral Pd@PdPt electrocatalysts integrating core–shell, alloy and concave structures for high-efficiency oxygen reduction and hydrogen evolution reactions. Journal of Materials Chemistry A, 2016, 4, 16690-16697.	10.3	69
46	Two-dimensional nanostructures of non-layered ternary thiospinels and their bifunctional electrocatalytic properties for oxygen reduction and evolution: the case of CuCo <sub>2</sub> S <sub>4</sub> nanosheets. Inorganic Chemistry Frontiers, 2016, 3, 1501-1509.	6.0	69
47	Preparation of lotus-leaf-like polystyrene micro- and nanostructure films and its blood compatibility. Journal of Materials Chemistry, 2009, 19, 9025.	6.7	68
48	A general strategy for embedding ultrasmall CoM <sub>x</sub> nanocrystals (M = S, O, Se, and Te) in hierarchical porous carbon nanofibers for high-performance potassium storage. Journal of Materials Chemistry A, 2021, 9, 1487-1494.	10.3	68
49	Ultralong Cycle Life Sodium-Ion Battery Anodes Using a Graphene-Templated Carbon Hybrid. Journal of Physical Chemistry C, 2014, 118, 22426-22431.	3.1	66
50	Self-assembly of a mesoporous ZnS/mediating interface/CdS heterostructure with enhanced visible-light hydrogen-production activity and excellent stability. Chemical Science, 2015, 6, 5263-5268.	7.4	65
51	Sn4P3 nanoparticles confined in multilayer graphene sheets as a high-performance anode material for potassium-ion batteries. Journal of Energy Chemistry, 2022, 66, 413-421.	12.9	64
52	Polarized Optoelectronics of CsPbX <sub>3</sub> (X = Cl, Br, I) Perovskite Nanoplates with Tunable Size and Thickness. Advanced Functional Materials, 2018, 28, 1800283.	14.9	63
53	Novel nitrogen-doped reduced graphene oxide-bonded Sb nanoparticles for improvedÂsodium storage performance. Journal of Materials Chemistry A, 2018, 6, 11244-11251.	10.3	62
54	Enhancing the Anode Performance of Antimony through Nitrogen-Doped Carbon and Carbon Nanotubes. Journal of Physical Chemistry C, 2016, 120, 3214-3220.	3.1	61

#	Article	lF	CITATIONS
55	Component-Controlled Synthesis of Necklace-Like Hollow Ni <sub><i>X</i></sub> Ru <sub><i>y</i></sub> Nanoalloys as Electrocatalysts for Hydrogen Evolution Reaction. ACS Applied Materials & Interfaces, 2017, 9, 17326-17336.	8.0	60
56	Construction of Metal-Ion-Free G-quadruplex-Hemin DNAzyme and Its Application in S1 Nuclease Detection. ACS Applied Materials & amp; Interfaces, 2016, 8, 827-833.	8.0	56
57	3D Porous Nanoarchitectures Derived from SnS/Sâ€Doped Graphene Hybrid Nanosheets for Flexible Allâ€Solidâ€State Supercapacitors. Small, 2017, 13, 1603494.	10.0	55
58	Engineering Mo/Mo <sub>2</sub> C/MoC hetero-interfaces for enhanced electrocatalytic nitrogen reduction. Journal of Materials Chemistry A, 2020, 8, 8920-8926.	10.3	54
59	Phaseâ€Modulation of Iron/Nickel Phosphides Nanocrystals "Armored―with Porous Pâ€Doped Carbon and Anchored on Pâ€Doped Graphene Nanohybrids for Enhanced Overall Water Splitting. Advanced Functional Materials, 2021, 31, 2010912.	14.9	54
60	Enabling Superior Electrochemical Properties for Highly Efficient Potassium Storage by Impregnating Ultrafine Sb Nanocrystals within Nanochannelâ€Containing Carbon Nanofibers. Angewandte Chemie, 2019, 131, 14720-14725.	2.0	53
61	Fabrication of Hierarchical Nanostructure of Silver via a Surfactant-Free Mixed Solvents Route. Crystal Growth and Design, 2009, 9, 3941-3947.	3.0	52
62	Arabinogalactan protein–rare earth element complexes activate plant endocytosis. Proceedings of the National Academy of Sciences of the United States of America, 2019, 116, 14349-14357.	7.1	52
63	A novel tetragonal pyramid-shaped porous ZnO nanostructure and its application in the biosensing of horseradish peroxidase. Journal of Materials Chemistry, 2008, 18, 1919.	6.7	51
64	Synergistic effect of mesoporous Mn <sub>2</sub> O <sub>3</sub> -supported Pd nanoparticle catalysts for electrocatalytic oxygen reduction reaction with enhanced performance in alkaline medium. Journal of Materials Chemistry A, 2014, 2, 1272-1276.	10.3	51
65	Quantum dots sensitized titanium dioxide decorated reduced graphene oxide for visible light excited photoelectrochemical biosensing at a low potential. Biosensors and Bioelectronics, 2014, 54, 331-338.	10.1	49
66	Crystalline Facet-Directed Generation Engineering of Ultrathin Platinum Nanodendrites. Journal of Physical Chemistry Letters, 2019, 10, 663-671.	4.6	49
67	Novel surfactant-directed synthesis of ultra-thin palladium nanosheets as efficient electrocatalysts for glycerol oxidation. Chemical Communications, 2017, 53, 1642-1645.	4.1	47
68	Fluorescence Regulation of Copper Nanoclusters via DNA Template Manipulation toward Design of a High Signal-to-Noise Ratio Biosensor. ACS Applied Materials & Interfaces, 2018, 10, 6965-6971.	8.0	47
69	A localized surface plasmon resonance-enhanced photoelectrochemical biosensing strategy for highly sensitive and scatheless cell assay under red light excitation. Chemical Communications, 2016, 52, 11799-11802.	4.1	45
70	Vertically Oriented and Interpenetrating CuSe Nanosheet Films with Open Channels for Flexible All-Solid-State Supercapacitors. ACS Omega, 2017, 2, 1089-1096.	3.5	45
71	Synthesis of multicore-shell FeS2@C nanocapsules for stable potassium-ion batteries. Journal of Energy Chemistry, 2022, 73, 126-132.	12.9	43
72	High-Performance Flexible In-Plane Micro-Supercapacitors Based on Vertically Aligned CuSe@Ni(OH) <sub>2</sub> Hybrid Nanosheet Films. ACS Applied Materials & Interfaces, 2018, 10, 38341-38349.	8.0	41

#	Article	IF	CITATIONS
73	Conjugated Polymer-Quantum Dot Hybrid Materials for Pathogen Discrimination and Disinfection. ACS Applied Materials & Interfaces, 2020, 12, 21263-21269.	8.0	41
74	Two-dimensional porous γ-AlOOH and γ-Al <sub>2</sub> O <sub>3</sub> nanosheets: hydrothermal synthesis, formation mechanism and catalytic performance. RSC Advances, 2015, 5, 71728-71734.	3.6	40
75	Allâ€Inorganic Perovskite Quantum Dots/pâ€5i Heterojunction Lightâ€Emitting Diodes under DC and AC Driving Modes. Advanced Optical Materials, 2018, 6, 1700897.	7.3	39
76	A "Signal On―Photoelectrochemical Biosensor Based on Bismuth@N,O odoped arbon Core‧hell Nanohybrids for Ultrasensitive Detection of Telomerase in HeLa Cells. Chemistry - A European Journal, 2018, 24, 3677-3682.	3.3	35
77	Engineering the Morphology and Configuration of Ternary Heterostructures for Improving Their Photocatalytic Activity. ACS Applied Materials & Interfaces, 2016, 8, 4516-4522.	8.0	34
78	Novel Blood-Compatible Polyurethane Ionomer Nanoparticles. Macromolecules, 2009, 42, 9366-9368.	4.8	32
79	Highly branched ultrathin Pt–Ru nanodendrites. Chemical Communications, 2019, 55, 11131-11134.	4.1	31
80	Facile synthesis of ultrathin single-crystalline palladium nanowires with enhanced electrocatalytic activities. Chemical Communications, 2016, 52, 12996-12999.	4.1	30
81	A novel nanostructure of nickel nanotubes encapsulated in carbon nanotubes. Chemical Communications, 2003, , 208-209.	4.1	29
82	Construction of Amorphous FePO <sub>4</sub> Nanosheets with Enhanced Sodium Storage Properties. ACS Applied Energy Materials, 2018, 1, 4395-4402.	5.1	29
83	Reversible Transformation between CsPbBr <sub>3</sub> Perovskite Nanowires and Nanorods with Polarized Optoelectronic Properties. Advanced Functional Materials, 2021, 31, 2011251.	14.9	29
84	A highly stable potassium-ion battery anode enabled by multilayer graphene sheets embedded with SnTe nanoparticles. Chemical Engineering Journal, 2022, 435, 135100.	12.7	29
85	Electrochemical monitoring of an important biomarker and target protein: VEGFR2 in cell lysates. Scientific Reports, 2014, 4, 3982.	3.3	28
86	Low Potential Detection of NADH at Titanium-Containing MCM-41â€Modified Glassy Carbon Electrode. Electroanalysis, 2007, 19, 604-607.	2.9	27
87	Componentâ€Controlled Synthesis of Smallâ€Sized Pdâ€Ag Bimetallic Alloy Nanocrystals and Their Application in a Nonâ€Enzymatic Glucose Biosensor. Particle and Particle Systems Characterization, 2013, 30, 549-556.	2.3	27
88	SbSI Nanocrystals: An Excellent Visible Light Photocatalyst with Efficient Generation of Singlet Oxygen. ACS Sustainable Chemistry and Engineering, 2018, 6, 12166-12175.	6.7	27
89	Polyoxometalateâ€Decorated gâ€C <sub>3</sub> N <sub>4</sub> â€Wrapping Snowflakeâ€Like CdS Nanocrystal for Enhanced Photocatalytic Hydrogen Evolution. Chemistry - A European Journal, 2018, 24, 15930-15936.	3.3	27
90	Significantly Enhanced Hydrogen Evolution Activity of Freestanding Pdâ€Ru Distorted Icosahedral Clusters with less than 600 Atoms. Chemistry - A European Journal, 2017, 23, 18203-18207.	3.3	24

	Jian-Chun Bao		
#	Article	IF	Citations
91	Sequence and Structure Dual-Dependent Interaction between Small Molecules and DNA for the Detection of Residual Silver Ions in As-Prepared Silver Nanomaterials. Analytical Chemistry, 2017, 89, 6815-6820.	6.5	23
92	Ligand-controlled synthesis of high density and ultra-small Ru nanoparticles with excellent electrocatalytic hydrogen evolution performance. Nano Research, 2022, 15, 1269-1275.	10.4	23
93	Synergistic effects of ZrO <sub>2</sub> or B <sub>2</sub> O <sub>3</sub> on flameâ€retarded poly (butyl) Ţ	j ETQ <sub>0</sub> 1 1 0. 2.0	784314 rgB <mark>T</mark> 22
94	Dual-path modulation of hydrogen peroxide to ameliorate hypoxia for enhancing photodynamic/starvation synergistic therapy. Journal of Materials Chemistry B, 2020, 8, 9933-9942.	5.8	22
95	Synergistic effects of nanoâ€Mn <sub>0.4</sub> Zn <sub>0.6</sub> Fe <sub>2</sub> O <sub>4</sub> on intumescent flameâ€retarded polypropylene. Journal of Vinyl and Additive Technology, 2008, 14, 120-125.	3.4	21
96	Well-Coupled Nanohybrids Obtained by Component-Controlled Synthesis and in Situ Integration of Mn <sub><i>x</i></sub> Pd <sub><i>y</i></sub> Nanocrystals on Vulcan Carbon for Electrocatalytic Oxygen Reduction. ACS Applied Materials & Interfaces, 2018, 10, 8155-8164.	8.0	20
97	Amorphous Y(OH) <sub>3</sub> -promoted Ru/Y(OH) <sub>3</sub> nanohybrids with high durability for electrocatalytic hydrogen evolution in alkaline media. Chemical Communications, 2018, 54, 12202-12205.	4.1	19
98	Nanostructured metal chalcogenides confined in hollow structures for promoting energy storage. Nanoscale Advances, 2020, 2, 583-604.	4.6	18
99	Anchoring ultrafine CoP and CoSb nanoparticles into rich N-doped carbon nanofibers for efficient potassium storage. Science China Materials, 2022, 65, 43-50.	6.3	18
100	Detection of NADH and Ethanol at Titanium Containing MCM-41 with Low Overpotential. Electroanalysis, 2007, 19, 1591-1596.	2.9	15
101	Polyoxometalate-assisted fabrication of the Pd nanoparticle/reduced graphene oxide nanocomposite with enhanced methanol-tolerance for the oxygen reduction reaction. New Journal of Chemistry, 2016, 40, 914-918.	2.8	15
102	<scp>Doubleâ€Coated Fe<sub>2</sub>N</scp> @ <scp>TiO<sub>2</sub></scp> @C <scp>Yolkâ€ShellSubmicrocubes as an Advanced Anode for <scp>Potassiumâ€ion</scp> Batteries<sup>â€</sup>. Chinese Journal of Chemistry, 2021, 39, 1878-1884.</scp>	> 4.9	15
103	CsPbX <sub>3</sub> â€ITO (X <b>=</b> Cl, Br, I) Nanoâ€Heterojunctions: Voltage Tuned Positive to Negative Photoresponse. Small, 2021, 17, e2101403.	10.0	15
104	Facile synthesis of PdFe alloy tetrahedrons for boosting electrocatalytic properties towards formic acid oxidation. Nanoscale, 2019, 11, 18015-18020.	5.6	14
105	Charge, adsorption, water stability and bandgap tuning of an anionic Cd( <scp>ii</scp> ) porphyrinic metal–organic framework. Dalton Transactions, 2019, 48, 8678-8692.	3.3	14
106	Versatile Synthesis of Pdâ^'M (M=Cr, Mo, W) Alloy Nanosheets Flowerâ€like Superstructures for Efficient Oxygen Reduction Electrocatalysis. ChemCatChem, 2020, 12, 4138-4148.	3.7	14
107	Monoclinic Copper(I) Selenide Nanocrystals and Copper(I) Selenide/Palladium Heterostructures: Synthesis, Characterization, and Surface-Enhanced Raman Scattering Performance. European Journal of Inorganic Chemistry, 2015, 2015, 2229-2236.	2.0	13
108	Unveiling the anti-cancer mechanism for half-sandwich and cyclometalated Ir(iii)-based complexes with functionalized α-lipoic acid. RSC Advances, 2020, 10, 5392-5398.	3.6	13

#	Article	IF	CITATIONS
109	Rapid Aqueous Synthesis of Large‣ize and Edge/Defectâ€Rich Porous Pd and Pdâ€Alloyed Nanomesh for Electrocatalytic Ethanol Oxidation. Chemistry - A European Journal, 2021, 27, 11175-11182.	3.3	12
110	A postsynthetic ion exchange method for tunable doping of hydroxyapatite nanocrystals. RSC Advances, 2017, 7, 56537-56542.	3.6	11
111	Mesoporous SiO2–(l)-lysine hybrid nanodisks: direct electron transfer of superoxide dismutase, sensitive detection of superoxide anions and its application in living cell monitoring. RSC Advances, 2013, 3, 20456.	3.6	10
112	Continuous preparation of antimony nanocrystals with near infrared photothermal property by pulsed laser ablation in liquids. Scientific Reports, 2020, 10, 15095.	3.3	9
113	Ambipolar Photoresponse of CsPbX <sub>3</sub> -ZnO (X = Cl, Br, and I) Heterojunctions. ACS Applied Electronic Materials, 2022, 4, 1525-1532.	4.3	9
114	General Preparation and Shaping of Multifunctional Nanowire Aerogels for Pressure/Gas/Photo-Sensing. Advanced Fiber Materials, 2022, 4, 66-75.	16.1	7
115	Ternary phase diagram of all-inorganic perovskite CsPbClaBrbI3â^'aâ^'b nanocrystals. Nano Research, 2022, 15, 7590-7596.	10.4	7
116	Synergistic Effects of Nano-BaWO <sub>4</sub> on Intumescent Flame-Retarded Polypropylene. Polymer-Plastics Technology and Engineering, 2009, 48, 621-626.	1.9	6
117	Small-sized Ag nanocrystals: high yield synthesis in a solid–liquid phase system, growth mechanism and their successful application in the Sonogashira reaction. RSC Advances, 2012, 2, 6061.	3.6	6
118	Correction to Two-Dimensional Tin Selenide Nanostructures for Flexible All-Solid-State Supercapacitors. ACS Nano, 2014, 8, 6509-6509.	14.6	6
119	Quantum Dots for Monitoring Choline Consumption Process of Living Cells via an Electrostatic Force-Mediated Energy Transfer. ACS Applied Bio Materials, 2019, 2, 5528-5534.	4.6	5
120	Two anionic Ni(II) porphyrinic metalâ^'organic frameworks: Syntheses, flexibility and roles in visible-light photocatalytic CO2 reduction to CO in the Ru(bpy)3Cl2/TEA/CH3CN system. Journal of Solid State Chemistry, 2020, 287, 121340.	2.9	5
121	Gramâ€Scale Synthesis of Multipod Pd Nanocrystals by a Simple Solid–Liquid Phase Reaction and Their Remarkable Electrocatalytic Properties. European Journal of Inorganic Chemistry, 2012, 2012, 3740-3746.	2.0	4
122	Overall Water Splitting: Cobalt Phosphides Nanocrystals Encapsulated by P-Doped Carbon and Married with P-Doped Graphene for Overall Water Splitting (Small 10/2019). Small, 2019, 15, 1970052.	10.0	4
123	The cocatalyst roles of three anionic Cd(II) porphyrinic metal-organic frameworks in the photocatalytic CO2 reduction to CO process carried out in Ru(bpy)3Cl2/CH3CN/H2O/Triethylamine or triethanolamine system. Journal of Solid State Chemistry, 2020, 292, 121690.	2.9	4
124	Engineering PdIr Nanostructures Synergistically Induced by Selfâ€assembled Surfactants and Halide Ions for Alcohol Electrooxidation. Chemistry - A European Journal, 2022, 28, .	3.3	4
125	Geometric bionics: Lotus effect helps polystyrene nanotube films get good blood compatibility. Nature Precedings, 2009, , .	0.1	3
126	Agar-induced hollow porous carbon nanospheres anchored platinum for high-performance hydrogenation. Chemosphere, 2020, 243, 125387.	8.2	3

#	Article	IF	CITATIONS
127	Theoretical Investigation into Thermodynamics and Electronic Structure of an Ammonia-productive Molybdenum-centered Catalyst. Inorganic Chemistry, 2021, 60, 11878-11882.	4.0	3
128	A nanoscaled Au–horseradish peroxidase composite fabricated by an interface reaction and its characterization, immobilization and biosensing. Analytical Methods, 2015, 7, 3466-3471.	2.7	1
129	Supercapacitors: 3D Porous Nanoarchitectures Derived from SnS/Sâ€Doped Graphene Hybrid Nanosheets for Flexible Allâ€Solidâ€State Supercapacitors (Small 12/2017). Small, 2017, 13, .	10.0	Ο